High-accuracy calculation of energies, lifetimes, hyperfine constants, multipole polarizabilities, and blackbody radiation shift in ^{39}K

U. I. Safronova[1,2] and M. S. Safronova[3]
[1]*Physics Department, University of Nevada, Reno, Nevada 89557, USA*
[2]*Institute of Spectroscopy, Russian Academy of Science, Troitsk, Moscow, Russia*
[3]*Department of Physics and Astronomy, 217 Sharp Lab, University of Delaware, Newark, Delaware 19716, USA*
(Received 12 September 2008; published 7 November 2008)

Excitation energies of the ns, np_j, nd_j, nf_j, and ng_j states with $n \leqslant 7$ in neutral potassium are evaluated. First-, second-, third-, and all-order Coulomb energies and first- and second-order Coulomb-Breit energies are calculated. Reduced matrix elements, oscillator strengths, transition rates, and lifetimes are determined for levels up to $n=9-12$. Electric-dipole ($4s_{1/2}$-np_j, $n=4-26$), electric-quadrupole ($4s_{1/2}$-nd_j, $n=3-26$), and electric-octupole ($4s_{1/2}$-nf_j, $n=4-26$) matrix elements are calculated to obtain the ground state E_1, E_2, and E_3 static polarizabilities. Scalar and tensor polarizabilities for the $4p_j$ excited state in K I are also calculated. All the above-mentioned matrix elements are determined using the all-order method. We also investigate the hyperfine structure in ^{39}K. The hyperfine A values are determined for the first low-lying levels up to $n=7$. The quadratic Stark effect on hyperfine structure levels of the ^{39}K ground state is investigated. The calculated shift for the $(F=2,M=0) \leftrightarrow (F=1,M=0)$ transition is found to be -0.0746 Hz/(kV/cm)^2, in agreement with the experimental value -0.071 ± 0.002 Hz/(kV/cm)^2. These calculations provide a theoretical benchmark for comparison with experiment and theory.

DOI: 10.1103/PhysRevA.78.052504 PACS number(s): 31.15.ac, 31.15.ag, 31.15.aj

I. INTRODUCTION

We report results of *ab initio* calculations of excitation energies, lifetimes, hyperfine constants, and polarizabilities in neutral potassium. The lifetime of the potassium $5p_{1/2}$ state was recently measured by pulsed excitation followed by nonresonant photoionization to monitor the state population [1]. The authors of this paper underlined that measurements of lifetimes of atomic alkali-metal states provide useful tests of many-body *ab initio* wave functions. Very recently, the theoretical and experimental values of the $5f$, $6f$, $7f$, and $8f$ radiative lifetimes of neutral potassium were reported [2]. The experiment was performed in a cell using time-resolved fluorescence spectroscopy. The nf states were excited stepwise, $4s \rightarrow 4p \rightarrow nf$, using two pulsed synchronous dye lasers for the dipole and quadrupole transitions, respectively. The reduced matrix elements for all allowed electric-dipole $nf_{5/2}$-$n'd_{5/2}$, $nf_{5/2}$-$n'd_{3/2}$, and $nf_{7/2}$-$n'd_{5/2}$ transitions with $n=5-8$ in K were calculated using the relativistic linearized coupled-cluster method with single and double excitations of Dirac-Fock wave functions included to all orders in many-body perturbation theory [2].

Relativistic many-body calculations of energy levels, hyperfine constants, electric-dipole matrix elements, and static polarizabilities for alkali-metal atoms were presented by Safronova *et al.* [3]. Only a few low-lying states were considered in that work [3]. In the present paper, the relativistic all-order method is used to calculate the atomic properties of neutral potassium for the ns, np_j, nd_j, nf_j, and ng_j ($n \leqslant 12$) states. We evaluate a large number of transition matrix elements to calculate lifetimes of the $ns_{1/2}$ ($n=5-12$), np_j ($n=4-12$), nd_j ($n=4-10$), and nf_j ($n=4-9$) states, and E_1, E_2, and E_3 ground-state polarizabilities.

Previously, the potassium atom has been studied in a number of experimental [4–29] and theoretical [30–42] papers. First experimental measurements were published more than 50 years ago by Stephenson [4]. The lifetimes of the $4p_{1/2,3/2}$ (27.1 ± 0.9 ns) states were measured using a magnetic rotation method. Some years later, the hyperfine structure of ^{39}K in the $4p_{1/2,3/2}$ states was measured using the atomic-beam magnetic resonance method [5]. Measurements of the electric polarizability of potassium were presented by Salon *et al.* in 1961 [8]. The atomic beam E-H gradient balance method was used in Ref. [8].

The radiative lifetimes of the $7s$-$11s$ and $5d$-$9d$ states of potassium measured by means of time- and wavelength-resolved laser-induced-fluorescence approaches were presented by Gallagher and Cooke [19]. Those measurements were repeated later by Hart and Atkinson [25]. In that paper, radiative lifetimes of the $6s$-$12s$, $3d$, and $5d$-$10d$ excited states in potassium were measured by time-resolved laser-induced fluorescence using two-photon excitation. Hart and Atkinson [25] noted that their results were systematically smaller than those of Gallagher and Cooke [19]. Precise determination of the dipole matrix elements and radiative lifetimes of the ^{39}K $4p_{1/2}$ and $4p_{3/2}$ states by photoassociative spectroscopy was presented recently by Wang *et al.* [28].

Hyperfine structure of the first excited $4p_{3/2}$ and $5p_{3/2}$ states of ^{39}K measured using the optical level-crossing method was presented by Schmieder *et al.* [11]. Cascade radio-frequency spectroscopy was used to determine the hyperfine structures of the excited $5s$ and $6s$ states of the stable potassium isotopes [14]. Using the optical double resonance and level crossing methods, the properties of several excited ($5d_j$, $6d_j$, $6p_j$, $7p_j$, $8s$, and $10s$) states in ^{39}K were studied by Belin *et al.* [17]. The ns and nd states were populated using stepwise excitation with the first np state used as an intermediate level [17]. Hyperfine quantum-beat spectroscopy was utilized in a pump-probe configuration to measure magnetic dipole (A) and electric quadrupole (B) coupling constants in the $3d_{3/2,5/2}$ levels of three isotopes of potassium (^{39}K, ^{40}K,

and ^{41}K) [27]. For many of these levels, the largest hyperfine splitting is smaller than the natural width, therefore a subnatural linewidth technique was used by Sieradzan *et al.* [27].

Measurements of the Stark shift of the $(F=2\ M=0)\leftrightarrow(F=1\ M=0)$ ground-state hyperfine interval in K were carried out by Snider [10] $[-0.0760\pm0.0076\ \mathrm{Hz/(kV/cm)^2}]$ and by Mowat [13] $[-0.071\pm0.002\ \mathrm{Hz/(kV/cm)^2}]$. The corresponding theoretical values were evaluated by Kelly *et al.* [31] $[-0.061\ \mathrm{Hz/(kV/cm)^2}]$ and by Lee *et al.* [32] $[-0.0683\ \mathrm{Hz/(kV/cm)^2}]$.

Dipole transition probabilities, oscillator strengths, lifetimes, and branching ratios derived from a numerical Coulomb approximation were presented by Lindgard and Nielsen [33] for the alkali-metal isoelectronic sequences from Li I up to Fr I. Modified Coulomb approximation with the effects of core polarization and spin-orbit interaction was used by Theodosiou [35] to evaluate lifetimes of alkali-metal atom Rydberg states. Fully relativistic model potential calculations were carried out by Migdalek and Kim to calculate oscillator strengths in neutral potassium, rubidium, and cesium [38]. In that paper, the authors demonstrated that the spin-orbit interaction cannot be solely responsible for the observed anomalous ratios of the oscillator strengths in those systems. They concluded that the anomalous ratios result from the interplay of spin-orbit interaction, core-valence electron correlation (core polarization), and cancellations in transition integrals.

One of the first high-precision *ab initio* calculations of atomic properties of alkali-metal atoms was presented by Johnson *et al.* [37]. Third-order many-body perturbation theory was used to obtain $E1$ transition amplitudes for ions of the lithium and sodium isoelectronic sequences and for the neutral alkali-metal atoms from potassium to francium. Complete angular reductions of the first-, second-, and third-order amplitudes were given. For neutral alkali-metal atoms, amplitudes of the $np_{1/2}\rightarrow ns_{1/2}$, $np_{3/2}\rightarrow ns_{1/2}$, $(n+1)s_{1/2}\rightarrow np_{1/2}$, and $(n+1)s_{1/2}\rightarrow np_{3/2}$ transitions, where n is the principal quantum number of the valence electron in the atomic ground state, were evaluated [37]. Ground- and excited-state energies, ionization potentials, and electron affinities were calculated for all the alkali-metal atoms using the relativistic Fock-space singles-doubles coupled-cluster (CCSD) method in Ref. [43]. High-accuracy calculation of the removal energies of Rb, Cs, Fr and element 119 was carried out in Ref. [44] using the CCSD method starting from Dirac-Coulomb-Breit Hamiltonian. We already mentioned above the relativistic many-body calculations of atomic properties for alkali-metal atoms presented by Safronova *et al.* [3]. Those calculations were carried out using the relativistic single-double (SD) method in which single and double excitations of Dirac-Fock wave functions are included to all orders of perturbation theory. Using SD wave functions, accurate values of removal energies, electric-dipole matrix elements, hyperfine constants, and static polarizabilities were obtained [3].

In the present work, we also use the relativistic single-double method, however we increase the number of basis-set orbitals up to 70 instead of 40 used in [3] to increase the number of states considered. We use B-splines [45] to generate a complete set of Dirac-Fock (DF) basis orbitals for use in the evaluation of all atomic properties. The present calculation of the lifetimes and polarizabilities required accurate representation of rather highly excited states, such as $6l_j$-$13l_j$, leading to the use of the large $R=220$ a.u. cavity for the generation of the finite basis set and higher number of splines to produce high-accuracy single-particle orbitals.

The main motivation for this work is to provide recommended values for a number of atomic properties via a systematic high-precision study for use in planning and analysis of various experiments as well as theoretical modeling. Another motivation is to study the methods to accelerate convergence of the all-order iterative scheme for the *nd* states. We have tested an approach that significantly reduced the time required for the calculation of the all-order excitation coefficients without loss of accuracy. Moreover, our tests demonstrate the improvement of the accuracy over the original scheme. Such a method is of importance to evaluating the properties of the *nd* states in heavy systems where the calculation time is significant or for a combination of the all-order and configuration-interaction methods where the calculations have to be carried out for a large number of states.

II. THIRD-ORDER AND ALL-ORDER CALCULATIONS OF ENERGIES

Energies of nl_j states in K I are evaluated for $n\leqslant 7$ and $l\leqslant 3$ using both third-order relativistic many-body perturbation theory (RMBPT) and the single-double (SD) all-order method discussed in Ref. [47], in which single and double excitations of Dirac-Fock (DF) wave functions are iterated to all orders. Results of our energy calculations are summarized in Table I. Columns 2-8 of Table I give the lowest-order DF energies $E^{(0)}$, second-order and third-order Coulomb correlation energies $E^{(2)}$ and $E^{(3)}$, first-order and second-order Breit corrections $B^{(1)}$ and $B^{(2)}$, and an estimated Lamb shift contribution, $E^{(\mathrm{LS})}$. The Lamb shift $E^{(\mathrm{LS})}$ is calculated as the sum of the one-electron self-energy and the first-order vacuum-polarization energy. The vacuum-polarization contribution is calculated from the Uehling potential using the results of Fullerton and Rinker [48]. The self-energy contribution is estimated for the s, $p_{1/2}$, and $p_{3/2}$ orbitals by interpolating among the values obtained by Mohr [49–51] using Coulomb wave functions. For this purpose, an effective nuclear charge Z_{eff} is obtained by finding the value of Z_{eff} required to give a Coulomb orbital with the same average $\langle r\rangle$ as the DF orbital. It should be noted that the values of $E^{(\mathrm{LS})}$ are very small. For states with $l>0$, the Lamb shift is estimated to be smaller than 0.1 $\mathrm{cm^{-1}}$ using scaled Coulomb values and is ignored. We list the all-order SD energies in the column labeled E^{SD} and list that part of the third-order energies missing from E^{SD} in the column labeled $E^{(3)}_{\mathrm{extra}}$. The sum of the seven terms $E^{(0)}$, E^{SD}, $E^{(3)}_{\mathrm{extra}}$, $B^{(1)}$, $B^{(2)}$, and $E^{(\mathrm{LS})}$ is our final all-order result $E^{\mathrm{SD}}_{\mathrm{tot}}$, listed in the eleventh column of Table I. Recommended energies from the National Institute of Standards and Technology (NIST) database [46] are given in the column labeled E_{NIST}. Differences between our third-order and all-order calculations and experimental data, $\delta E^{(3)}=E^{(3)}_{\mathrm{tot}}-E_{\mathrm{NIST}}$ and $\delta E^{\mathrm{SD}}=E^{\mathrm{SD}}_{\mathrm{tot}}-E_{\mathrm{NIST}}$, are given in the two final columns of Table I, respectively.

TABLE I. Zeroth-order (DF), second-, and third-order Coulomb correlation energies $E^{(n)}$, single-double Coulomb energies E^{SD}, $E^{(3)}_{\mathrm{extra}}$, first-order Breit, and second-order Coulomb-Breit corrections $B^{(n)}$ to the energies of K I. The total energies ($E^{(3)}_{\mathrm{tot}}=E^{(0)}+E^{(2)}+E^{(3)}+B^{(1)}+B^{(2)}+E^{(\mathrm{LS})}$, $E^{\mathrm{SD}}_{\mathrm{tot}}=E^{(0)}+E^{\mathrm{SD}}+E^{(3)}_{\mathrm{extra}}+B^{(1)}+B^{(2)}+E^{(\mathrm{LS})}$) for K I are compared with experimental energies E_{NIST} [46], $\delta E=E_{\mathrm{tot}}-E_{\mathrm{NIST}}$. Units: cm^{-1}.

nlj	$E^{(0)}$	$E^{(2)}$	$E^{(3)}$	$B^{(1)}$	$B^{(2)}$	$E^{(\mathrm{LS})}$	$E^{(3)}_{\mathrm{tot}}$	E^{SD}	$E^{(3)}_{\mathrm{extra}}$	$E^{\mathrm{SD}}_{\mathrm{tot}}$	E_{NIST}	$\delta E^{(3)}$	δE^{SD}
$4s_{1/2}$	−32370	−2734.0	449.3	8.6	−10.3	0.9	−34656	−2887.1	291.1	−34967	−35010	354	43
$4p_{1/2}$	−21006	−1012.8	136.7	4.6	−3.3	0.0	−21881	−1119.4	102.0	−22023	−22025	143	2
$4p_{3/2}$	−20959	−1000.6	134.9	3.3	−3.6	0.0	−21825	−1105.6	100.7	−21965	−21967	142	2
$3d_{3/2}$	−12744	−608.6	88.0	0.5	−2.3	0.0	−13267	−764.1	60.7	−13450	−13473	206	23
$3d_{5/2}$	−12747	−608.5	87.9	0.3	−2.3	0.0	−13270	−763.8	60.6	−13452	−13475	205	23
$4d_{3/2}$	−7205	−337.9	53.6	0.4	−1.6	0.0	−7491	−426.8	33.7	−7600	−7612	121	12
$4d_{5/2}$	−7207	−337.7	53.5	0.2	−1.5	0.0	−7492	−426.3	33.6	−7601	−7613	120	12
$4f_{5/2}$	−6859	−22.5	1.5	0.0	0.0	0.0	−6880	−24.2	2.3	−6881	−6882	2	1
$4f_{7/2}$	−6859	−22.5	1.5	0.0	0.0	0.0	−6880	−24.2	2.3	−6881	−6882	2	1
$5s_{1/2}$	−13407	−628.0	109.1	2.3	−2.6	0.1	−13926	−621.0	68.0	−13960	−13983	57	23
$5p_{1/2}$	−10012	−304.5	43.9	1.6	−1.2	0.0	−10272	−322.8	30.8	−10304	−10308	36	5
$5p_{3/2}$	−9996	−301.2	43.4	1.2	−1.3	0.0	−10254	−319.4	30.4	−10285	−10290	36	5
$5d_{3/2}$	−4596	−191.8	31.4	0.2	−1.0	0.0	−4757	−240.6	19.1	−4818	−4824	67	6
$5d_{5/2}$	−4597	−191.6	31.4	0.1	−0.9	0.0	−4758	−240.1	19.1	−4819	−4825	67	6
$5f_{5/2}$	−4390	−12.9	0.9	0.0	0.0	0.0	−4402	−13.9	1.3	−4403	−4403	1	1
$5f_{7/2}$	−4390	−12.9	0.9	0.0	0.0	0.0	−4402	−13.9	1.3	−4403	−4403	1	1
$5g_{7/2}$	−4389	−3.1	0.2	0.0	0.0	0.0	−4392	−3.3	0.3	−4392	−4392	0	0
$6s_{1/2}$	−7338	−244.5	43.2	0.9	−1.1	0.0	−7540	−237.1	26.6	−7549	−7559	20	10
$6p_{1/2}$	−5882	−134.0	19.7	0.7	−0.5	0.0	−5996	−137.6	13.6	−6005	−6011	15	5
$6p_{3/2}$	−5874	−132.7	19.5	0.5	−0.6	0.0	−5987	−136.2	13.4	−5997	−6002	15	5
$6d_{3/2}$	−3177	−116.3	19.4	0.1	−0.6	0.0	−3274	−144.8	11.6	−3310	−3314	40	3
$6d_{5/2}$	−3177	−116.2	19.3	0.1	−0.6	0.0	−3275	−144.5	11.6	−3311	−3314	39	3
$6f_{5/2}$	−3049	−7.9	0.6	0.0	0.0	0.0	−3056	−8.5	0.8	−3056	−3057	1	0
$6f_{7/2}$	−3049	−7.9	0.6	0.0	0.0	0.0	−3056	−8.5	0.8	−3056	−3057	1	0
$6g_{7/2}$	−3048	−2.0	0.1	0.0	0.0	0.0	−3050	−2.1	0.2	−3050			
$7s_{1/2}$	−4627	−120.5	21.5	0.5	−0.5	0.0	−4727	−115.8	13.1	−4730	−4736	9	5
$7p_{1/2}$	−3872	−71.0	10.5	0.4	−0.3	0.0	−3932	−73.7	7.2	−3938	−3940	8	2
$7p_{3/2}$	−3868	−70.3	10.4	0.3	−0.3	0.0	−3928	−73.0	7.1	−3934	−3935	8	2
$7d_{3/2}$	−2324	−75.8	12.7	0.1	−0.4	0.0	−2387	−93.4	7.6	−2410	−2411	24	1
$7d_{5/2}$	−2324	−75.7	12.7	0.1	−0.4	0.0	−2387	−93.2	7.5	−2410	−2412	24	1
$7f_{5/2}$	−2240	−5.2	0.4	0.0	0.0	0.0	−2245	−5.5	0.5	−2245	−2245	0	0
$7f_{7/2}$	−2240	−5.2	0.4	0.0	0.0	0.0	−2245	−5.5	0.5	−2245	−2245	0	0
$7g_{7/2}$	−2240	−1.3	0.1	0.0	0.0	0.0	−2241	−1.44	0.1	−2241			

As expected, the largest correlation contribution to the valence energy comes from the second-order term $E^{(2)}$. Therefore, we calculate $E^{(2)}$ with higher numerical accuracy. The second-order energy includes partial waves up to $l_{\mathrm{max}}=8$ and is extrapolated to account for contributions from higher partial waves (see, for example, Refs. [52,53] for details of the extrapolation procedure). As an example of the convergence of $E^{(2)}$ with the number of partial waves l, consider the $4s_{1/2}$ state. Calculations of $E^{(2)}$ with $l_{\mathrm{max}}=6$ and 8 yield $E^{(2)}(4s_{1/2})=-2717.8$ and $-2727.4\ \mathrm{cm}^{-1}$, respectively. Extrapolation of these calculations yields −2734.0 and $-2734.2\ \mathrm{cm}^{-1}$, respectively. Thus, in this particular case, we have a numerical uncertainty in $E^{(2)}(4s_{1/2})$ of $0.2\ \mathrm{cm}^{-1}$. It should be noted that the $16.7\ \mathrm{cm}^{-1}$ contribution from partial waves with $l>6$ for the $4s$ state is the largest among all states considered in Table I; smaller (about $4-6\ \mathrm{cm}^{-1}$) contributions are obtained for the $3d$, $4p$, and $4d$ states and much smaller contributions ($0.5-1.5\ \mathrm{cm}^{-1}$) are obtained for $n=5$ states.

Owing to numerical complexity, we restrict $l\leqslant l_{\mathrm{max}}=6$ in the E^{SD} calculation. As noted above, the second-order contribution dominates E^{SD}; therefore, we can use the extrapolated value of the $E^{(2)}$ described above to account for the contributions of the higher partial waves. Six partial waves are also used in the calculation of $E^{(3)}$. Since the asymptotic l dependences of the second- and third-order energies are similar (both fall off as l^{-4}), we use the second-order remainder as a guide to estimate the remainder in the third-order

TABLE II. Reduced electric-dipole matrix elements calculated to first, second, third, and all orders of RMBPT in K I.

Transition		$Z^{(DF)}$	$Z^{(DF+2)}$	$Z^{(DF+2+3)}$	$Z^{(SD)}$
$4s_{1/2}$	$4p_{1/2}$	4.5546	4.3979	4.0834	4.0982
$4s_{1/2}$	$4p_{3/2}$	6.4391	6.2186	5.7727	5.7939
$4p_{1/2}$	$4d_{3/2}$	0.7691	0.6960	0.2805	0.1137
$4p_{3/2}$	$4d_{3/2}$	0.3359	0.3036	0.1154	0.0403
$4p_{3/2}$	$4d_{5/2}$	1.0028	0.9055	0.3417	0.1177
$3d_{3/2}$	$4p_{1/2}$	8.5962	8.4667	7.9969	3.5569
$3d_{3/2}$	$4p_{3/2}$	3.8546	3.7966	3.5873	3.5569
$3d_{5/2}$	$4p_{3/2}$	11.5637	11.3896	10.7616	10.6708

contribution. The term $E^{(3)}_{extra}$ in Table I, which accounts for that part of the third-order MBPT energy missing from the SD expression for the energy, is smaller than $E^{(3)}$ by an order of magnitude for the states considered here.

The column labeled δE^{SD} in Table I gives differences between our *ab initio* results and the experimental values [46]. The SD results agree better with measured values than do the third-order MBPT results (the ratio of $\delta E^{(3)}/\delta E^{SD}$ is about 10 for some of cases), illustrating the importance of fourth- and higher-order correlation corrections.

III. ELECTRIC-DIPOLE MATRIX ELEMENTS, OSCILLATOR STRENGTHS, TRANSITION RATES, AND LIFETIMES IN NEUTRAL POTASSIUM

A. Electric-dipole matrix elements

The calculation of the transition matrix elements provides another test of the quality of atomic-structure calculations and another measure of the size of correlation corrections. Reduced electric-dipole matrix elements between low-lying states of K I calculated in the third-order RMBPT and in the all-order SD approximation are presented in Table II. We include only a limited number of transitions in this table to illustrate our results.

Our calculations of reduced matrix elements in the lowest, second, and third orders are carried out following the method described in Ref. [55]. The lowest-order DF values labeled $Z^{(DF)}$ are given in the third column of Table II. The values $Z^{(DF+2)}$ are obtained as the sum of the second-order correlation correction $Z^{(2)}$ and the DF matrix elements $Z^{(DF)}$. It should be noted that the second-order Breit correction $B^{(2)}$ is rather small in comparison with the second-order Coulomb correction $Z^{(2)}$ (the ratio of $B^{(2)}$ to $Z^{(2)}$ is about 1–2 %).

The third-order matrix elements $Z^{(DF+2+3)}$ include the DF values, the second-order $Z^{(2)}$ results, and the third-order $Z^{(3)}$ correlation correction. $Z^{(3)}$ includes random-phase-approximation terms (RPA) iterated to all orders, Brueckner orbital (BO) corrections, structural radiation $Z^{(SR)}$, and normalization $Z^{(NORM)}$ terms (see [56] for definition of these terms).

The terms $Z^{(RPA)}$ and $Z^{(BO)}$ give the largest contributions to $Z^{(3)}$. The sum of terms $Z^{(RPA)}$ and $Z^{(BO)}$ is about 10% of the $Z^{(DF)}$ term and has a different sign for the $4s$-$4p$ and $3d$-$4p$ transitions. The value of $Z^{(BO)}$ becomes the largest contribution for the $4p$-$4d$ transitions and decreases the value of $Z^{(DF+2+3)}$ by a factor of 2 in comparison with the $Z^{(DF)}$ term. The structural radiation $Z^{(SR)}$ and normalization $Z^{(NORM)}$ terms are small. All results given in Table II are obtained using the length form of the matrix elements. Length-form and velocity-form matrix elements differ typically by 5–20 % for the DF matrix elements and 2–5 % for the second-order matrix elements in these calculations.

Electric-dipole matrix elements evaluated in the all-order SD approximation are given in columns labeled $Z^{(SD)}$ of Table II. The SD matrix elements $Z^{(SD)}$ include $Z^{(3)}$ completely, along with important fourth- and higher-order corrections. The fourth-order corrections omitted from the SD matrix elements were discussed recently in [57]. The $Z^{(SD)}$ values are smaller than the $Z^{(DF+2)}$ values and larger than the $Z^{(DF+2+3)}$ values for some transitions given in Table II.

To obtain the all-order matrix elements, we first need to calculate the all-order excitation coefficients using an iterative procedure [3]. The correlation contributions to matrix elements are linear of quadratic functions of the excitation coefficients. The iteration procedure is terminated when the relative change in the correlation energy in two consecutive iterations is sufficiently small (10^{-5} in the present calculations). While the *ns* and *np* state calculations require just a few iterations, the iterative procedure for the *nd* state in general converges very slowly requiring over 20 iterations owing to large correlation corrections leading to large oscillations of energy values in subsequent iterations. The resulting values of energies are also in relatively poor agreement with experiment, again, owing to large correlation corrections from excluded triple- and higher-excitation terms. The correlation corrections for most of the transition properties of the *nd* states are dominated by the term containing the single valence excitation coefficients that are closely related to the correlation energy [58]. In fact, it has been demonstrated (see [58–60] and references therein), that scaling of the single excitation coefficients with the exact correlation energy value (i.e., multiplying the single valence excitation coefficients ρ_{mv} by the ratio of the "experimental" to corresponding theoretical correlation energy values and recalculating the matrix element values with modified coefficients) leads to more precise results. Therefore, if the excitation coefficients correspond to accurate energies, the corresponding transition matrix elements involving *nd* states are expected to be more accurate. To verify this statement, we have made two different calculations for the *nd* states. First, we continued iteration until the energy sufficiently converged (after 23 iterations). Secondly, we stopped the iteration procedure at the point where the correlation energy is the closest to its experimental value, which happens after only three iterations owing to large oscillations of the energy values. We note that each iteration essentially picks up one more order of perturbation theory in each correlation term. We note that the energy after three iterations is much closer to the experimental value than the final result. Finally, we carried out the scaling procedure of the single excitation coefficients in both cases. A summary of these results and comparison with the recommended values obtained from the experimental Stark shifts in Ref. [54] for the $4p$-$3d$ transitions is given in Table III.

TABLE III. Comparison of the $3d$-$4p$ electric-dipole matrix elements obtained with different values of the all-order excitation coefficients. The three iterations correspond to nearly experimental value of the correlation energy. The 23 iterations yield fully converged all-order SD results. The corresponding scaled data are given in columns labeled SD_{sc}. The SDpT *ab initio* calculations partially include triple excitations. The results are compared with the recommended values obtained from the Stark shift data in Ref. [54].

Transition	SD	SD	SD_{sc}	SD_{sc}	SDpT	Ref. [54]
	3 iter.	23 iter.	3 iter.	23 iter.		
$3d_{3/2}$-$4p_{1/2}$	7.930	7.868	7.971	7.949	7.956	7.984
$3d_{3/2}$-$4p_{3/2}$	3.557	3.529	3.575	3.565	3.568	3.580
$3d_{5/2}$-$4p_{3/2}$	10.671	10.587	10.724	10.696	10.708	10.741

This table confirms our earlier supposition that ending the iteration procedure at the correct energy value would produce more accurate results for the transition properties of the *nd* states, while significantly reducing the required computation time.

B. Transition rates, oscillator strengths, and line strengths in potassium

Transition rates $A_r(s^{-1})$, oscillator strengths (f), and line strengths S (a.u.) for the $4p_j$-ns, $4p_j$-$nd_{j'}$, $3d_j$-$np_{j'}$, and $3d_j$-$nf_{j'}$ transitions in K I calculated in the SD approximation are summarized in Table IV. To provide recommended values for these properties, we carried out the scaling procedure described above where appropriate. We use recommended NIST energies [46] in the calculation of the transition rates A_r and oscillator strengths f. In Table IV, we divide transitions into groups according to the initial state for better presentation. We evaluate the $4s$-np_j and $4p_j$-ns transitions with n up to $n=13$, the $3d_j$-$np_{j'}$ transitions up to $n=12$, the $4p_j$-$nd_{j'}$ transitions up to $n=11$, and the $3d_j$-$nf_{j'}$ transitions up to $n=9$. In all these cases, we check the quality of our functions created in an $R=220$ a.u. cavity with $N=70$ splines by comparing the nl_j-$nl'_{j'}$ dipole matrix elements evaluated using the B-spline basis-set orbitals and directly obtained DF values.

C. Lifetimes in potassium

We calculate the lifetimes of the $ns_{1/2}$ ($n=5-12$), np_j ($n=4-12$), nd_j ($n=3-10$), and nf_j ($n=4-9$) states in potassium using the SD results for dipole matrix elements and NIST data for energies [46]. We list lifetimes $\tau^{(SD)}$ obtained by the SD method in Table V and compare our values with available experimental [1,2,11,25,26,28] and theoretical [3,35] results. We also quote the SD scaled data where appropriate. We find that while the scaling significantly modifies certain small matrix elements, it does not significantly change *ab initio* lifetimes.

We already mentioned that the first lifetime measurements were published more than 50 years ago by Stephenson [4]. The lifetimes of the $4p_{1/2,3/2}$ (27.1 ± 0.9 ns) states were measured using a magnetic rotation method. Almost 50 years later, photoassociative spectroscopy was used to determine the lifetimes of the $4p_{1/2,3/2}$ states [28]. New results are $\tau(4p_{1/2})=26.69\pm0.05$ ns and $\tau(4p_{3/2})=26.34\pm0.05$ ns. The two sets of measurements of the *ns* and *nd* lifetimes by Gallagher and Cooke [19] and by Hart and Atkinson [25] have slightly different error bars. In Table V, we use measurements from Ref. [25] since they were the most recent ones. The radiative lifetimes of the fine-structure components of the $5p$, $6p$, and $7p$ states in potassium determined using techniques of laser-induced fluorescence were presented by Berends *et al.* [26]; these values are used in our table. Finally, experimental values of the $5f$, $6f$, $7f$, and $8f$ radiative lifetimes of neutral potassium reported recently in Ref. [2] were included in the experimental set of Table V.

The last column of Table V (labeled τ^{th}) lists other available theoretical lifetimes. Results given by Hart and Atkinson [25] and Theodosiou [35] were obtained using the modified Coulomb approximation. Relativistic all-order values were presented by Safronova *et al.* [3] and Glódź *et al.* [2].

Our SD results are in excellent agreement with experimental results when experimental uncertainties are taken into account. The largest disagreement (about 15%) is between τ^{SD} and τ^{expt} for the $5d_{3/2}$ and $6d_{3/2}$ states. However, our τ^{SD} value agrees better with the τ^{expt} value for the $6d_{3/2}$ state than the τ^{th} value presented in the same paper as the τ^{expt} value [25]. We find similar comparisons for the $7d_{3/2}$, $8d_{3/2}$, and $9d_{3/2}$ states. We already mentioned previously that for the np-$n'd$ transitions, the value of $Z^{(BO)}$ becomes very large and decreases the value of $Z^{(DF+2+3)}$ by a factor of 2 in comparison with the $Z^{(DF)}$ term. In these cases, triple excitations become important and need to be taken into account to improve results.

IV. STATIC MULTIPOLE POLARIZABILITIES OF THE 4*s* GROUND STATE OF NEUTRAL K

The static multipole polarizability α^{Ek} of K in its $4s$ ground state can be separated into two terms: a dominant first term from intermediate valence-excited states, and a smaller second term from intermediate core-excited states. The latter term is smaller than the former one by several orders of magnitude and is evaluated here in the random-phase approximation [62]. The dominant valence contribution is calculated using the sum-over-state approach,

$$\alpha_v^{Ek}=\frac{1}{2k+1}\sum_n\frac{|\langle nl_j\|r^kC_{kq}\|4s\rangle|^2}{E_{nlj}-E_{4s}}, \tag{1}$$

where $C_{kq}(\hat{r})$ is a normalized spherical harmonic and where nl_j is np_j, nd_j, and nf_j for $k=1$, 2, and 3, respectively [63].

TABLE IV. Wavelengths λ (Å), transition rates A_r (s^{-1}), oscillator strengths (f), and line strengths S (a.u.) for transitions in K I calculated using the all-order method; scaling is included for transition to states with n up to $n=7$. Numbers in brackets represent powers of 10.

Transition		λ	A_r	f	S	Transition		λ	A_r	f	S
$4p_{1/2}$	$5s_{1/2}$	12435.7	7.95[6]	1.84[−1]	1.51[1]	$3d_{3/2}$	$5p_{1/2}$	31601.6	1.65[6]	1.23[−1]	5.13[1]
$4p_{1/2}$	$6s_{1/2}$	6913.0	2.50[6]	1.79[−2]	8.16[−1]	$3d_{3/2}$	$6p_{1/2}$	13400.7	4.47[5]	6.02[−3]	1.06[0]
$4p_{1/2}$	$7s_{1/2}$	5784.0	1.19[6]	5.95[−3]	2.27[−1]	$3d_{3/2}$	$7p_{1/2}$	10490.0	2.17[5]	1.79[−3]	2.47[−1]
$4p_{1/2}$	$8s_{1/2}$	5324.8	6.64[5]	2.82[−3]	9.90[−2]	$3d_{3/2}$	$8p_{1/2}$	9354.1	1.24[5]	8.13[−4]	1.00[−1]
$4p_{1/2}$	$9s_{1/2}$	5085.6	4.09[5]	1.59[−3]	5.31[−2]	$3d_{3/2}$	$9p_{1/2}$	8769.5	7.79[4]	4.49[−4]	5.19[−2]
$4p_{1/2}$	$10s_{1/2}$	4943.4	2.70[5]	9.89[−4]	3.22[−2]	$3d_{3/2}$	$10p_{1/2}$	8422.3	5.23[4]	2.78[−4]	3.08[−2]
$4p_{1/2}$	$3d_{3/2}$	11693.4	2.01[7]	8.25[−1]	6.35[1]	$3d_{3/2}$	$5p_{3/2}$	31415.4	1.66[5]	2.46[−2]	1.02[1]
$4p_{1/2}$	$4d_{3/2}$	6938.2	1.90[4]	2.75[−4]	1.26[−2]	$3d_{3/2}$	$6p_{3/2}$	13385.6	4.54[4]	1.22[−3]	2.15[−1]
$4p_{1/2}$	$5d_{3/2}$	5813.8	2.86[5]	2.90[−3]	1.11[−1]	$3d_{3/2}$	$7p_{3/2}$	10485.0	2.21[4]	3.64[−4]	5.02[−2]
$4p_{1/2}$	$6d_{3/2}$	5344.5	3.86[5]	3.30[−3]	1.16[−1]	$3d_{3/2}$	$8p_{3/2}$	9351.8	1.26[4]	1.65[−4]	2.03[−2]
$4p_{1/2}$	$7d_{3/2}$	5098.6	3.39[5]	2.64[−3]	8.87[−2]	$3d_{3/2}$	$9p_{3/2}$	8768.1	7.92[3]	9.13[−5]	1.05[−2]
$4p_{1/2}$	$8d_{3/2}$	4952.2	2.79[5]	2.05[−3]	6.69[−2]	$3d_{3/2}$	$10p_{3/2}$	8421.5	5.31[3]	5.65[−5]	6.27[−3]
$4p_{3/2}$	$5s_{1/2}$	12525.6	1.58[7]	1.86[−1]	3.06[1]	$3d_{5/2}$	$5p_{3/2}$	31392.7	1.50[6]	1.48[−1]	9.15[1]
$4p_{3/2}$	$6s_{1/2}$	6940.7	4.95[6]	1.79[−2]	1.63[0]	$3d_{5/2}$	$6p_{3/2}$	13381.5	4.11[5]	7.36[−3]	1.95[0]
$4p_{3/2}$	$7s_{1/2}$	5803.4	2.35[6]	5.93[−3]	4.53[−1]	$3d_{5/2}$	$7p_{3/2}$	10482.5	1.99[5]	2.18[−3]	4.52[−1]
$4p_{3/2}$	$8s_{1/2}$	5341.2	1.31[6]	2.81[−3]	1.98[−1]	$3d_{5/2}$	$8p_{3/2}$	9349.8	1.14[5]	9.92[−4]	1.83[−1]
$4p_{3/2}$	$9s_{1/2}$	5100.6	8.10[5]	1.58[−3]	1.06[−1]	$3d_{5/2}$	$9p_{3/2}$	8766.4	7.14[4]	5.48[−4]	9.49[−2]
$4p_{3/2}$	$10s_{1/2}$	4957.5	5.34[5]	9.84[−4]	6.43[−2]	$3d_{5/2}$	$10p_{3/2}$	8419.8	4.79[4]	3.39[−4]	5.64[−2]
$4p_{3/2}$	$3d_{3/2}$	11772.9	3.97[6]	8.24[−2]	1.28[1]	$3d_{3/2}$	$4f_{5/2}$	15172.5	1.45[7]	7.51[−1]	1.50[2]
$4p_{3/2}$	$4d_{3/2}$	6966.1	2.40[3]	1.75[−5]	1.60[−3]	$3d_{3/2}$	$5f_{5/2}$	11025.7	6.10[6]	1.67[−1]	2.42[1]
$4p_{3/2}$	$5d_{3/2}$	5833.3	6.13[4]	3.13[−4]	2.40[−2]	$3d_{3/2}$	$6f_{5/2}$	9600.4	3.21[6]	6.65[−2]	8.41[0]
$4p_{3/2}$	$6d_{3/2}$	5361.0	8.06[4]	3.47[−4]	2.45[−2]	$3d_{3/2}$	$7f_{5/2}$	8906.5	1.91[6]	3.41[−2]	4.00[0]
$4p_{3/2}$	$7d_{3/2}$	5113.6	7.02[4]	2.75[−4]	1.85[−2]						
$4p_{3/2}$	$8d_{3/2}$	4966.4	5.76[4]	2.13[−4]	1.39[−2]	$3d_{5/2}$	$4f_{5/2}$	15167.2	1.04[6]	3.57[−2]	1.07[1]
						$3d_{5/2}$	$5f_{5/2}$	11022.9	4.36[5]	7.94[−3]	1.73[0]
$4p_{3/2}$	$3d_{5/2}$	11776.1	2.38[7]	7.42[−1]	1.15[2]	$3d_{5/2}$	$6f_{5/2}$	9598.3	2.29[5]	3.17[−3]	6.00[−1]
$4p_{3/2}$	$4d_{5/2}$	6966.6	1.37[4]	1.49[−4]	1.37[−2]	$3d_{5/2}$	$7f_{5/2}$	8904.6	1.37[5]	1.63[−3]	2.86[−1]
$4p_{3/2}$	$5d_{5/2}$	5833.5	3.71[5]	2.84[−3]	2.18[−1]						
$4p_{3/2}$	$6d_{5/2}$	5361.1	4.86[5]	3.14[−3]	2.22[−1]	$3d_{5/2}$	$4f_{7/2}$	15167.2	1.55[7]	7.15[−1]	2.14[2]
$4p_{3/2}$	$7d_{5/2}$	5113.7	4.23[5]	2.49[−3]	1.67[−1]	$3d_{5/2}$	$5f_{7/2}$	11022.9	6.54[6]	1.59[−1]	3.46[1]
$4p_{3/2}$	$8d_{5/2}$	4966.4	3.46[5]	1.92[−3]	1.26[−1]	$3d_{5/2}$	$6f_{7/2}$	9598.3	3.44[6]	6.33[−2]	1.20[1]
						$3d_{5/2}$	$7f_{7/2}$	8904.6	2.05[6]	3.25[−2]	5.72[0]

The reduced matrix elements in the above sum are evaluated using the SD approximation for basis states with $n \leqslant 26$, and in the DF approximation for the remaining states, scaling is included into $E2$ and $E3$ matrix elements.

Contributions to dipole, quadrupole, and octupole polarizabilities of the $4s$ ground state are presented in Table VI. The first two terms in the sum over states for α^{E1}, α^{E2}, and α^{E3} contribute 99.6%, 95.1%, and 44.6%, respectively, of the totals. The rapid convergence of the sum over states for α^{E1} has been emphasized in many publications (for example, Refs. [3,40]). We use recommended energies from [46] and SD wave functions to evaluate terms in the sum with $n \leqslant 13$, and we use theoretical SD energies and wave functions to evaluate terms with $13 \leqslant n \leqslant 26$. The remaining contributions to α^{Ek} from basis functions with $27 \leqslant n \leqslant 70$ are evaluated in the DF approximation. As one can see from Table VI, sums over n for $n \leqslant 26$ in α^{E2} and α^{E3} essentially reproduce the final results, since the contributions from $27 \leqslant n \leqslant 70$ are smaller than 0.01% in all cases.

Final results for the multipole polarizabilities of the ground state K I are compared in Table VI with high-precision calculations given in Refs. [40,61] and experimental measurements presented in Refs. [15,16]. Scaled values (SD_{sc}) are included to provide recommended values for the $E2$ and $E3$ polarizabilities. Our results agree with values given by Derevianko *et al.* [40] for the dipole polarizability taking into account the uncertainty given in [40]. The uncertainty in the experimental measurements [15,16] of the dipole polarizability is too large to reflect on the accuracy of the present calculations. Scaled values (SD_{sc}) are included to

TABLE V. Lifetimes (in ns) of nl_j states in neutral potassium. The SD ($\tau^{(SD)}$) and SD scaled ($\tau^{(SD_{sc})}$) values are compared with theoretical and experimental data.

Level	$\tau^{(DF)}$	$\tau^{(SD)}$	$\tau^{(SD_{sc})}$	τ^{expt}	τ^{th}
$5s_{1/2}$	40.3	42.5	42.1		42.5 [3]
$6s_{1/2}$	78.2	81.4	81.3	88 ± 2 [25]	88 [25]
$7s_{1/2}$	143.4	148.8	149.0	155 ± 6 [25]	158 [25]
$8s_{1/2}$	241.6	250.7		238 ± 4 [25]	264 [25]
$9s_{1/2}$	379.3	393.6		384 ± 14 [25]	414 [25]
$10s_{1/2}$	563.2	584.7		575 ± 26 [25]	614 [25]
$11s_{1/2}$	797.4	828.9		783 ± 50 [25]	872 [25]
$12s_{1/2}$	982.0	1034.6		1148 ± 42 [25]	1191 [25]
$4p_{1/2}$	21.7	26.8		26.69 ± 0.05 [28]	26.8 [3]
$4p_{3/2}$	21.5	26.5		26.34 ± 0.05 [28]	26.5 [3]
$5p_{1/2}$	116.2	137.1	137.2	137.6 ± 1.3 [1]	127.06 [35]
$5p_{3/2}$	113.6	133.9	134.0	134 ± 2 [26]	124.02 [35]
$6p_{1/2}$	295.0	340.7	342.2	344 ± 3 [26]	321.67 [35]
$6p_{3/2}$	287.7	332.0	333.8	333 ± 3 [26]	312.77 [35]
$7p_{1/2}$	589.3	648.6	649.3	623 ± 6 [26]	619.80 [35]
$7p_{3/2}$	573.9	632.0	633.2	592 ± 6 [26]	601.80 [35]
$8p_{1/2}$	1037.5	1077.2			1040.23 [35]
$8p_{3/2}$	1009.2	1050.2			1010.51 [35]
$9p_{1/2}$	1675.7	1652.0			1607.54 [35]
$9p_{3/2}$	1628.3	1611.2			1561.31 [35]
$10p_{1/2}$	2538.9	2397.6			2345.84 [35]
$10p_{3/2}$	2464.8	2338.9			2279.41 [35]
$11p_{1/2}$	3610.4	3293.8			3267.54 [35]
$11p_{3/2}$	3501.0	3212.9			3173.43 [35]
$12p_{1/2}$	4323.6	3791.2			4402.92 [35]
$12p_{3/2}$	4178.8	3691.7			4279.78 [35]
$3d_{3/2}$	35.7	41.9	41.5	42 ± 3 [25]	39 [25]
$3d_{5/2}$	36.2	42.5	42.0		45.85 [35]
$4d_{3/2}$	218.7	289.4	287.9		285.86 [35]
$4d_{5/2}$	223.9	293.9	292.5		291.18 [35]
$5d_{3/2}$	732.7	653.1	658.4	572 ± 14 [25]	579 [25]
$5d_{5/2}$	751.5	650.8	656.5		
$6d_{3/2}$	1567.9	925.7		807 ± 20 [25]	1085 [25]
$6d_{5/2}$	1597.2	913.7			
$7d_{3/2}$	2605.3	1231.9		1201 ± 26 [25]	1403 [25]
$7d_{5/2}$	2633.1	1212.7			
$8d_{3/2}$	3820.2	1627.0		1533 ± 80 [25]	1742 [25]
$8d_{5/2}$	3838.0	1600.3			
$9d_{3/2}$	5239.7	2127.1		2000 ± 140 [25]	2151 [25]
$9d_{5/2}$	5242.7	2091.7			
$10d_{3/2}$	6491.1	2586.3		2268 ± 146 [25]	2808 [25]
$10d_{5/2}$	6474.6	2542.8			
$4f_{5/2}$	48.3	64.7	64.0		70.65 [35]
$4f_{7/2}$	48.3	64.7	63.9		70.65 [35]
$5f_{5/2}$	93.7	118.0	116.9	117 ± 3 [2]	117 ± 4 [2]
$5f_{7/2}$	93.7	117.9	116.9		
$6f_{5/2}$	161.8	194.9	193.6	190 ± 6 [2]	195 ± 4 [2]
$6f_{7/2}$	161.8	194.9	193.5		
$7f_{5/2}$	257.6	300.4		300 ± 8 [2]	301 ± 6 [2]
$7f_{7/2}$	257.6	300.3			
$8f_{5/2}$	385.2	439.0		428 ± 10 [2]	441 ± 9 [2]
$8f_{7/2}$	385.1	438.8			
$9f_{5/2}$	547.3	616.1			638.03 [35]
$9f_{7/2}$	547.1	615.8			637.93 [35]

provide recommended values for the $E2$ and $E3$ polarizabilities. The scaling is expected to provide more accurate results since the dominant contributions to the relevant matrix elements come from the single valence excitation coefficients. Our recommended values for the quadrupole and octupole polarizabilities are in agreement with values of Ref. [61].

V. SCALAR AND TENSOR POLARIZABILITIES OF THE 4*p* EXCITED STATES OF K

The scalar $\alpha_0(v)$ and tensor $\alpha_2(v)$ polarizabilities of an excited state v of K are given by

$$\alpha_0(v) = \frac{2}{3(2j_v+1)} \sum_{nlj} \frac{|\langle v\|rC_1\|nlj\rangle|^2}{E_{nlj} - E_v}, \tag{2}$$

$$\alpha_2(v) = (-1)^{j_v} \sqrt{\frac{40j_v(2j_v-1)}{3(j_v+1)(2j_v+1)(2j_v+3)}} \times \sum_{nlj} (-1)^j \begin{Bmatrix} j_v & 1 & j \\ 1 & j_v & 2 \end{Bmatrix} \frac{|\langle v\|rC_1\|nlj\rangle|^2}{E_{nlj} - E_v}. \tag{3}$$

As before, our calculation of the sums is divided into three parts. The first part is the sum over valence states with $n \leqslant 26$, which is carried out using SD wave functions. The second part is the sum over basis states with $n > 26$, which is carried out in the DF approximation. The third part is the contribution from core-excited states, which is carried out in the random-phase approximation (RPA).

A breakdown of contributions to the scalar dipole polarizability for the excited $4p_{1/2}$ and $4p_{3/2}$ states is presented in Table VII. Contributions from the excited ns and nd states with $n \leqslant 26$ differ only by 0.001%. Contributions from excited ns and nd states $n > 26$ are very small—$\alpha_{n>26}(4p_{1/2}) = 0.075a_0^3$, $\alpha_{n>26}(4p_{3/2}) = 0.097a_0^3$—and are calculated in the DF approximation. We evaluate the contribution from ionic core α_{core} in the RPA and find $\alpha_{core} = 5.457a_0^3$. A counter term $\alpha_{vc}(4p_j)$ compensating for excitation from the core to the valence shell which violates the Pauli principle is also evaluated in the RPA and found to be $\alpha_{vc}(4p_j) = -0.000\,15a_0^3$. The above values were combined to obtain our final result for the scalar polarizabilities of the first two excited states in K I: $\alpha_0^{(SD)}(4p_{1/2}) = 604.1a_0^3$ and $\alpha_0^{(SD)}(4p_{3/2}) = 614.1a_0^3$.

We present details of our calculation of the tensor polarizability α_2 of the $4p_{3/2}$ state in Table VIII. Reduced electric-

TABLE VI. Contributions to multipole polarizabilities (a.u.) of the $4s$ state of potassium. The two leading terms and those terms with $n \leqslant 26$ in the expression for α_v^{Ek} [Eq. (1)] are evaluated using SD wave functions. The remainders ($n > 26$), labeled "tail" below, are evaluated in the DF approximation. Contributions from core-excited states α_c^{Ek} are evaluated in the random-phase approximation. Our final polarizabilities α^{E1}, α^{E2}, and α^{E3} of the $4s$ ground state of K are compared with other calculations and with experiment. Scaled values (SD_{sc}) are included to provide recommended values for the $E2$ and $E3$ polarizabilities.

$E1$ polarizability		$E2$ polarizability			$E3$ polarizability		
	SD		SD	SD_{sc}		SD	SD_{sc}
$nlj=4p_{1/2}$	94.6	$nlj=3d_{3/2}$	1861	1904	$nlj=4f_{5/2}$	32830	34429
$nlj=4p_{3/2}$	188.3	$nlj=3d_{5/2}$	2791	2857	$nlj=4f_{7/2}$	43774	45906
$nl=[5p\text{-}26p]$	1.0	$nl=[4d\text{-}26d]$	241	241	$nl=[5f\text{-}26f]$	95077	96679
tail	−0.1	tail	0	0	tail	12	12
α_v^{E1}	283.8	α_v^{E2}	4893	5002	α_v^{E3}	171693	177026
α_c^{E1}	5.5	α_c^{E2}	16	16	α_c^{E3}	110	110
Total α^{E1}	289.3	Total α^{E2}	4910	5018	Total α^{E3}	171802	177136
Ref. [40] (theor.)	290.2 ± 0.8	Ref. [61] (theor.)		5000 ± 45	Ref. [61] (expt.)		177000
Ref. [16] (expt.)	292.8 ± 6.1						
Ref. [15] (expt.)	305.0 ± 21.6						

dipole matrix elements evaluated in the SD approximation are given in columns labeled . The corresponding contributions to the tensor polarizability are given in columns labeled I_{nlj}. The sum of contributions from the $nd_{3/2}$ and $ns_{1/2}$ intermediate states is almost compensated for by the contribution from the $nd_{5/2}$ states. The resulting contribution to $\alpha_2(4p_{3/2})$ comes from states with $n \leqslant 26$ and is equal to $-107.9a_0^3$. Contributions from states with $n > 26$ give $-0.005a_0^3$.

States with $n > 13$ in our basis have positive energies and provide a discrete representation of the continuum. We find that the continuous part of spectra is responsible for 2% of $\alpha_2(4p_{3/2})$. We evaluated the continuum contributions in the range $14 < n \leqslant 26$ using SD wave functions for dipole matrix elements and energies. For $n \leqslant 13$, we use SD matrix elements and NIST energies [46] in the sums. Our final result is $\alpha_2^{(SD)}(4p_{3/2}) = -107.9a_0^3$.

Our results for scalar and tensor polarizabilities of the $4p_j$ excited states of potassium are compared with calculations in [30,39] and with experimental measurements reported by Marrus and Yellin [12] in Table IX. The Bates-Damgaard method was used by Schmieder *et al.* [30] and the time-dependent gauge-invariant variational method was used by Mérawa and Bégué [39]. The uncertainty in the experimental measurement [12] of the scalar polarizability is too large to reflect on the accuracy of the present calculations.

TABLE VII. Contributions to scalar polarizability of potassium in the excited $4p_{1/2}$ and $4p_{3/2}$ states calculated with SD wave functions; $\alpha_0(4p_{1/2}) = \Sigma_{n=3}^{70} I_{4p_{1/2}}(nd_{3/2}) + \Sigma_{n=1}^{70} I_{4p_{1/2}}(ns_{1/2})$, $\alpha_0(4p_{3/2}) = \Sigma_{n=3}^{70} I_{4p_{3/2}}(nd_j) + \Sigma_{n=1}^{70} I_{4p_{3/2}}(ns_{1/2})$.

Contribution	$j=1/2$	$j=3/2$
$\Sigma_{n=3}^{26} I_{4p_j}^{(SD)}(nd_{3/2})$	549.80	55.69
$\Sigma_{n=3}^{26} I_{4p_j}^{(SD)}(nd_{5/2})$	0	500.49
$\Sigma_{n=1}^{26} I_{4p_j}^{(SD)}(ns_{1/2})$	48.75	52.36
$\alpha_{main}^{(SD)}(4p_j)$	598.55	608.54
$\alpha_{tail}^{(DF)}(4p_j)$	0.07	0.10
$\alpha_{core}(4p_j)$	5.46	5.46
$\alpha_{vc}(4p_j)$	0.00	0.00
$\alpha^{(SD)}(4p_j)$	604.1	614.1

VI. HYPERFINE CONSTANTS FOR ^{39}K

Calculations of hyperfine constants follow the pattern described earlier for calculations of transition matrix elements. We find that the triple excitations are important for the hyperfine constants, so we conduct another all-order calculation with partial inclusion of the triple excitations; these results are referred to as SDpT values. In Table X, we list hyperfine constants A for ^{39}K and compare our values with available experimental data from Refs. [18,24,27,29].

In this table, we present the lowest-order $A^{(DF)}$ and all-order $A^{(SD)}$ values for the ns, np, and nd levels up to $n=7$. The magnetic moment and nuclear spin of ^{39}K used here are taken from [64]. Our SDpT results are in very good agreement with experimental results for the ns and $np_{1/2}$ states when experimental uncertainties are taken into account.

The correlation correction for the $nd_{5/2}$ states is of the same order of magnitude as the DF value and has an opposite sign. With such large cancellations, it is difficult to calculate $A(nd_{5/2})$ accurately. It should be noted that only for the $A(6d_{5/2})$ value do we have perfect agreement with measurements given in [24] when experimental uncertainties are taken into account. Our SD results agree with experimental measurements $A(nd_{5/2})$ [27] for $A(3d_{5/2})$, however they disagree with sign. The sign of $A(5d_{5/2})$ in Ref. [18] is uncertain. We did not find any experimental measurements for $A(4d_{5/2})$ hyperfine constant.

Finally, we would like to demonstrate very smooth dependence of the $A^{(SD)}(nlj)$ hyperfine constants from principal

TABLE VIII. Contributions to tensor polarizability of K in the excited state $v=4p_{3/2}$ calculated using the all-order SD method $\alpha_2(4p_{3/2})=\Sigma_{n=3}^{70} I_{4p_{3/2}}(nd_j)+\Sigma_{n=1}^{70} I_{4p_{3/2}}(ns_{1/2})$. SD dipole matrix elements $Z_{vn}=\langle v\|rC_1\|nlj\rangle$ are also given. All values are in a.u.

n	Z_{vn}	$I_v(nd_{3/2})$	n	Z_{vn}	$I_v(nd_{5/2})$	n	Z_{vn}	$I_v(ns_{1/2})$
$3d_{3/2}$	3.557	43.587	$3d_{5/2}$	10.671	−98.097			
$4d_{3/2}$	0.040	0.003	$4d_{5/2}$	0.118	−0.007	$4s_{1/2}$	5.794	94.145
$5d_{3/2}$	0.157	0.042	$5d_{5/2}$	−0.473	−0.095	$5s_{1/2}$	5.509	−139.076
$6d_{3/2}$	0.159	0.040	$6d_{5/2}$	−0.478	−0.090	$6s_{1/2}$	1.279	−4.155
$7d_{3/2}$	0.138	0.029	$7d_{5/2}$	−0.416	−0.065	$7s_{1/2}$	0.674	−0.965
$8d_{3/2}$	0.118	0.020	$8d_{5/2}$	0.355	−0.046	$8s_{1/2}$	0.445	−0.386
$9d_{3/2}$	0.101	0.015	$9d_{5/2}$	−0.304	−0.033	$9s_{1/2}$	0.326	−0.198
$10d_{3/2}$	0.091	0.012	$10d_{5/2}$	0.272	−0.026	$10s_{1/2}$	0.254	−0.117
$11d_{3/2}$	0.096	0.013	$11d_{5/2}$	0.289	−0.029	$11s_{1/2}$	0.206	−0.075
$12d_{3/2}$	−0.109	0.016	$12d_{5/2}$	0.326	−0.036	$12s_{1/2}$	0.181	−0.057
$13d_{3/2}$	0.119	0.019	$13d_{5/2}$	0.359	−0.043	$13s_{1/2}$	−0.190	−0.063
$14d_{3/2}$	−0.118	0.018	$14d_{5/2}$	0.377	−0.047	$14s_{1/2}$	0.206	−0.072
$15d_{3/2}$	−0.139	0.025	$15d_{5/2}$	0.460	−0.068	$15s_{1/2}$	−0.199	−0.066
$16d_{3/2}$	−0.047	0.003	$16d_{5/2}$	−0.247	−0.019	$16s_{1/2}$	−0.170	−0.047
$17d_{3/2}$	−0.238	0.070	$17d_{5/2}$	−0.747	−0.170	$17s_{1/2}$	−0.335	−0.181
$18d_{3/2}$	−0.058	0.004	$18d_{5/2}$	0.013	0.000	$18s_{1/2}$	−0.006	0.000
$19d_{3/2}$	0.316	0.113	$19d_{5/2}$	0.982	−0.269	$19s_{1/2}$	−0.509	−0.380
$20d_{3/2}$	0.381	0.145	$20d_{5/2}$	−1.155	−0.327	$20s_{1/2}$	0.538	−0.350
$21d_{3/2}$	0.306	0.078	$21d_{5/2}$	−0.048	0.000	$21s_{1/2}$	0.003	0.000
$22d_{3/2}$	0.405	0.140	$22d_{5/2}$	1.203	−0.298	$22s_{1/2}$	−0.472	−0.202
$23d_{3/2}$	0.374	0.096	$23d_{5/2}$	−1.095	−0.200	$23s_{1/2}$	−0.360	−0.081
$24d_{3/2}$	−0.297	0.047	$24d_{5/2}$	−0.853	−0.095	$24s_{1/2}$	−0.251	−0.026
$25d_{3/2}$	−0.198	0.016	$25d_{5/2}$	−0.557	−0.031	$25s_{1/2}$	0.179	−0.008
$26d_{3/2}$	−0.104	0.003	$26d_{5/2}$	−0.282	−0.006	$26s_{1/2}$	0.070	−0.001
Sum		44.556			−100.097			−52.361
					$\alpha_{n\leq 26}^{(\mathrm{SD})}(4p_{3/2})=-107.902$			
					$\alpha_{n>26}(4p_{3/2})=-0.005$			
					$\alpha^{(\mathrm{SD})}(4p_{3/2})=-107.907$			

quantum number n. In Fig. 1, we present our $A^{(\mathrm{SD})}(nlj)$ values for the $ns_{1/2}$, $np_{1/2}$, $np_{3/2}$, $nd_{3/2}$, and $nd_{5/2}$ levels with $n=4-13$. It should be noted that the values of $A^{(\mathrm{SD})}(nd_{5/2})$ are shown with opposite sign since we use a logarithmic scale.

VII. HYPERFINE-INDUCED TRANSITION POLARIZABILITY OF THE ^{39}K GROUND STATE

We now turn to the calculation of the quadratic Stark shift of the ground-state hyperfine interval $(F=2-F=1)$ in ^{39}K.

TABLE IX. Scalar (α_0) and tensor (α_2) polarizabilities of the excited $4p$ state in K I. The SD data are compared with theoretical and experimental values. All values are in atomic units.

	$\alpha^{(\mathrm{SD})}$	α_{theor}	α_{expt}
$\alpha_2(4p\ ^2P_{3/2})$	−107.9	−96 [30]	
$\alpha_0(4p\ ^2P_{1/2})$	604.1		587(87) [12]
$\alpha_0(4p\ ^2P_{3/2})$	614.1	635 [30]	613(103) [12]
$\alpha_0(4p\ ^2P)$	610.8	697.4 [39]	

The quadratic Stark shift is closely related to the blackbody radiation shift discussed, for example, in Refs. [47,65], and our calculation follows the procedure outlined in [47].

The dominant second-order contribution to the polarizability difference between the two hyperfine components of the $4s$ state cancels and, therefore, the Stark shift of the hyperfine interval is governed by the third-order F-dependent polarizability $\alpha_F^{(3)}(0)$. The expression for the $\alpha_F^{(3)}(0)$ has been given in [65]

$$\alpha_F^{(3)}(0)=\frac{1}{3}\sqrt{(2I)(2I+1)(2I+2)}\begin{Bmatrix} j_v & I & F \\ I & j_v & 1 \end{Bmatrix} \times g_I\mu_n(-1)^{F+I+j_v}(2T+C+R), \tag{4}$$

where g_I is the nuclear gyromagnetic ratio, μ_n is the nuclear magneton equal to $0.392\,465\,8\mu_B$ in ^{39}K, $I=3/2$ is the nuclear spin, and $j_v=1/2$ is the total angular momentum of the atomic ground state. The F-independent sums for T, C, and R ($|v\rangle\equiv|4s_{1/2}\rangle$) are given by Eqs. (5)–(7) by Beloy *et al.* [65].

TABLE X. Hyperfine constants A (in MHz) in ^{39}K ($I=3/2$, $\mu=0.391\,465\,8$ [64]). The SD and SDpT (single-double all-order method including partial triple excitations) data are compared with experimental results.

Level	$A^{(\mathrm{DF})}$	$A^{(\mathrm{SD})}$	$A^{(\mathrm{SDpT})}$	$A^{(\mathrm{expt})}$
$4s\ ^2S_{1/2}$	146.91	237.40	228.57	230.8598601(3) [18]
$4p\ ^2P_{1/2}$	16.616	28.689	27.662	27.775(42) [29]
$4p\ ^2P_{3/2}$	3.233	6.213	5.989	6.093(25) [29]
$3d\ ^2D_{3/2}$	0.447	0.983	1.111	0.96(4) [27]
$3d\ ^2D_{5/2}$	0.192	−0.535	−0.639	0.62(4) [27]
$4d\ ^2D_{3/2}$	0.281	0.678		
$4d\ ^2D_{5/2}$	0.120	−0.307		
$5s\ ^2S_{1/2}$	38.877	56.102	54.817	55.50(60) [18]
$5p\ ^2P_{1/2}$	5.735	9.202	8.949	9.02(17) [18]
$5p\ ^2P_{3/2}$	1.117	1.988	1.932	1.969(13) [18]
$5d\ ^2D_{3/2}$	0.168	0.409		0.44(10) [18]
$5d\ ^2D_{5/2}$	0.072	−0.167		$4\pm0.24(7)$ [18]
$6s\ ^2S_{1/2}$	15.759	22.025	21.609	21.81(18) [18]
$6p\ ^2P_{1/2}$	2.629	4.066	4.014	4.05(7) [18]
$6p\ ^2P_{3/2}$	0.512	0.874	0.866	0.886(8) [18]
$6d\ ^2D_{3/2}$	0.105	0.253		0.25(1) [24]
$6d\ ^2D_{5/2}$	0.0448	−0.0975		−0.12(4) [24]
$7s\ ^2S_{1/2}$	7.900	10.876	10.690	10.79(5) [18]
$7p\ ^2P_{1/2}$	1.417	2.191	2.140	2.18(5) [18]
$7p\ ^2P_{3/2}$	0.276	0.473	0.462	0.49(4) [18]
$7d\ ^2D_{3/2}$	0.0685	0.1644		
$7d\ ^2D_{5/2}$	0.0293	−0.0611		
$8s\ ^2S_{1/2}$	4.511	6.156	6.057	5.99(8) [18]
$9s\ ^2S_{1/2}$	2.814	3.818	3.759	
$10s\ ^2S_{1/2}$	1.871	2.529	2.491	2.41(5) [18]

We note first that the values of T, C, and R in atomic units are

$$2T^{\mathrm{DF}} = 8.7506 \times 10^{-4}, \quad C^{\mathrm{DF}} = 5.6279 \times 10^{-7},$$

$$R^{\mathrm{DF}} = 1.2095 \times 10^{-3} \tag{5}$$

in the DF approximation.

Since the value of C^{DF} is smaller than the T^{DF} and R^{DF} by three orders of magnitude, we did not recalculate the C term in the SD approximation.

The expression for R is similar to the one for $\alpha^{E1}(0)$ [compare Eq. (1) and the expression for R in [65]]. The difference is an additional factor of the diagonal hyperfine matrix element,

$$\langle 4s_{1/2}\|T\|4s_{1/2}\rangle^{(\mathrm{SD})} = 1.693 \times 10^{-7}\ \text{a.u.}$$

We evaluate matrix elements $\langle v\|rC_1\|n\rangle$ in the SD approximation for $n\leqslant 26$. We use recommended NIST energies [46] for n up to $n=13$ and SD energies for $14\leqslant n\leqslant 26$. The sum of terms for $n\leqslant 26$ is $R_{n\leqslant 26}=1.179\times 10^{-3}$. The remainder of the sum, evaluated in the DF approximation, $R_{n>26}=1.0\times 10^{-10}$, is negligible.

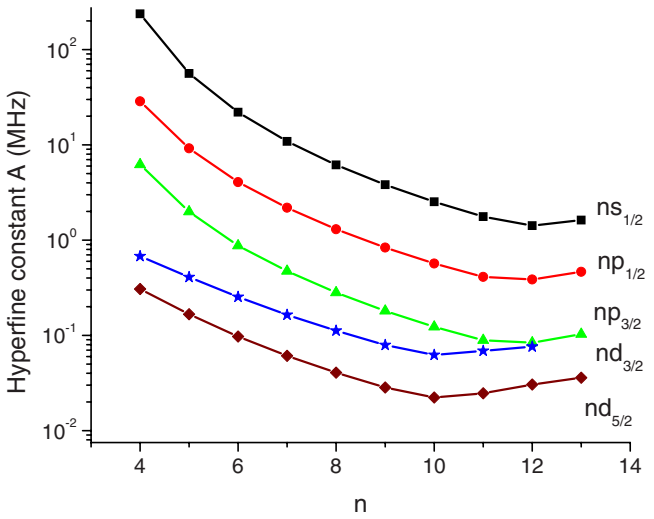

FIG. 1. (Color online) Hyperfine constant $A^{(\mathrm{SD})}(nlj)$ as a function of n.

The expression for T includes sums over two indices m and n. To calculate the dominant part of T, we limit the sum over m to six states ($m=4p_{1/2}$, $4p_{3/2}$, $5p_{1/2}$, $5p_{3/2}$, $6p_{1/2}$, and $6p_{3/2}$) and sum over n up to $n=26$,

$$T^{m\leqslant 3}_{n\leqslant 26} = -\frac{1}{2}\sum_{ns=5s}^{26s}\frac{\langle ns\|T^{(1)}\|4s\rangle}{(E_{ns}-E_{4s})} \times\left[\frac{\langle 4s\|rC_1\|4p_{1/2}\rangle\langle 4p_{1/2}\|rC_1\|ns\rangle}{(E_{4p_{1/2}}-E_{4s})} - \frac{\langle 4s\|rC_1\|4p_{3/2}\rangle\langle 4p_{3/2}\|rC_1\|ns\rangle}{(E_{4p_{3/2}}-E_{4s})} + \frac{\langle 4s\|rC_1\|5p_{1/2}\rangle\langle 5p_{1/2}\|rC_1\|ns\rangle}{(E_{5p_{1/2}}-E_{4s})} - \frac{\langle 4s\|rC_1\|5p_{3/2}\rangle\langle 5p_{3/2}\|rC_1\|ns\rangle}{(E_{5p_{3/2}}-E_{4s})} + \frac{\langle 4s\|rC_1\|6p_{1/2}\rangle\langle 6p_{1/2}\|rC_1\|ns\rangle}{(E_{6p_{1/2}}-E_{4s})} - \frac{\langle 4s\|rC_1\|6p_{3/2}\rangle\langle 6p_{3/2}\|rC_1\|ns\rangle}{(E_{6p_{3/2}}-E_{4s})}\right]. \tag{6}$$

The sum of the six contributions from Eq. (6) is 9.307×10^{-4}. The ratios of contributions to the sum from the $4p$ to $5p$ states and $5p$ to $6p$ are equal to 46 and 5, respectively. The relatively small remainder $T-T^{m>6}_{n>26}=-0.002\,98\times 10^{-4}$ is evaluated in the DF approximation, leading to a final value $T^{(\mathrm{SD})}=9.304\times 10^{-4}$. Combining these contributions, we obtain

$$2T^{\mathrm{SD}} + C^{\mathrm{DF}} + R^{\mathrm{SD}} = 2.110 \times 10^{-3}\ \text{a.u.} \tag{7}$$

The F-dependent factor [see Eq. (4)]

TABLE XI. Comparison of values of k in 10^{-10} Hz/(V/m)^2.

		References
Present	−0.07464	
Expt.	-0.0760 ± 0.0076	[10]
Expt.	-0.071 ± 0.002	[13]
Theory	−0.061	[31]
Theory	−0.0683	[32]

$$A(F) = \frac{g_I \mu_n}{3} \sqrt{(2I)(2I+1)(2I+2)} \times \begin{Bmatrix} j_v & I & F \\ I & j_v & 1 \end{Bmatrix} (-1)^{F+I+j_v}$$

is equal to −0.177 572 for $F=1$ and 0.106 543 for $F=2$. Using these values and the result from Eq. (7), we obtain

$$\alpha^{(3)}_{F=2}(0) - \alpha^{(3)}_{F=1}(0) = 5.9960 \times 10^{-4} \text{ a.u.}$$

The Stark shift coefficient k defined as $\Delta\nu = kE^2$ is $k = -\frac{1}{2}[\alpha^{(3)}_{F=2}(0) - \alpha^{(3)}_{F=1}(0)]$. Converting from atomic units, we obtain

$$k^{(\mathrm{SD})} = -2.9980 \times 10^{-4} \text{ a.u.} = -7.4600 \times 10^{-12} \text{ Hz/(V/m)}^2.$$

In the DF approximation [Eq. (5)], we find $k^{(\mathrm{DF})} = -7.3705 \times 10^{-12}$Hz/(V/m)^2.

In Table XI, we compare our SD value of k with available theoretical [31,32] and experimental [10,13] results. Our SD result is in better agreement with the experimental measurements than with theoretical results. It should be noted that the perturbation theory was used in both papers [31,32], however electron correlations were not included, as was underlined by [31].

The relative blackbody radiative shift β is defined as

$$\beta = -\frac{2}{15} \frac{1}{\nu_{\mathrm{hf}}} (\alpha\pi)^3 T^4 \alpha_{\mathrm{hf}}(4s_{1/2}), \tag{8}$$

where ν_{hf} is the ^{39}K hyperfine ($F=2$ and 1) splitting equal to 461.719 720 2 MHz and T is a temperature equal to 300 K. Using those factors, we can rewrite Eq. (8) as

$$\beta = -1.865 \times 10^{-11} \alpha_{\mathrm{hf}}(4s_{1/2}). \tag{9}$$

Using the SD value for $\alpha_{\mathrm{hf}}(4s_{1/2}) = 5.996 \times 10^{-4}$ a.u., we obtain finally

$$\beta^{(\mathrm{SD})} = -1.118 \times 10^{-14}. \tag{10}$$

VIII. CONCLUSION

In summary, a systematic RMBPT study of the energies of the $ns_{1/2}$, np_j, nd_j, and nf_j ($n \leqslant 6$) states in neutral potassium is presented. The energy values are in excellent agreement with existing experimental data. A systematic relativistic MBPT study of reduced matrix elements, oscillator strengths, transition rates, and lifetimes for the first low-lying levels up to $n=7$ is conducted. Electric-dipole ($4s_{1/2}$-np_j, $n=4-26$), electric-quadrupole ($4s_{1/2}$-nd_j, $n=3-26$), and electric-octupole ($4s_{1/2}$-nf_j, $n=4-26$) matrix elements are calculated to obtain the ground state $E1$, $E2$, and $E3$ static polarizabilities. Scalar and tensor polarizabilities for the $4p_j$ excited state in K I are calculated including $4p_j$-nd_j and $4p_j$-ns_j matrix elements with high n up to $n=26$. All of the above-mentioned matrix elements are determined using the all-order method. Hyperfine A values are presented for the first low-lying levels up to $n=7$. The quadratic Stark shift of the ground-state hyperfine interval in ^{39}K I is also evaluated. These calculations provide a theoretical benchmark for comparison with experiment and theory.

ACKNOWLEDGMENT

The work of M.S.S. was supported in part by National Science Foundation Grant No. PHY-07-58088.

[1] A. Mills, J. A. Behr, L. A. Courneyea, and M. R. Pearson, Phys. Rev. A **72**, 024501 (2005).
[2] M. Glódź, A. Huzandrov, M. S. Safronova, I. Sydoryk, J. Szonert, and J. Klavins, Phys. Rev. A **77**, 022503 (2008).
[3] M. S. Safronova, W. R. Johnson, and A. Derevianko, Phys. Rev. A **60**, 4476 (1999).
[4] G. Stephenson, Proc. Phys. Soc., London, Sect. A **64**, 458 (1951).
[5] P. Buck and I. I. Rabi, Phys. Rev. **107**, 1291 (1957).
[6] G. J. Ritter and G. Series, Proc. R. Soc. London, Ser. A **239**, 473 (1957).
[7] W. N. Fox and G. Series, Proc. Phys. Soc. London **77**, 1141 (1961).
[8] A. Salop, E. Polaack, and B. Bederson, Phys. Rev. **124**, 1431 (1961).
[9] G. E. Chamberlain and J. C. Zorn, Phys. Rev. **129**, 677 (1963).
[10] J. L. Snider, Phys. Lett. **21**, 172 (1966).
[11] R. W. Schmieder, A. Lurio, and W. Happer, Phys. Rev. **173**, 76 (1968).
[12] R. Marrus and J. Yellin, Phys. Rev. **177**, 127 (1969).
[13] J. R. Mowat, Phys. Rev. A **5**, 1059 (1972).
[14] R. Gupta, W. Happer, L. K. Lam, and S. Svanberg, Phys. Rev. A **8**, 2792 (1973).
[15] W. D. Hall and J. C. Zorn, Phys. Rev. A **10**, 1141 (1974).
[16] R. W. Molof, H. L. Schwartz, T. M. Miller, and B. Bederson, Phys. Rev. A **10**, 1131 (1974).
[17] G. Belin, L. Holmgren, I. Lindgren, and S. Svanberg, Phys. Scr. **12**, 287 (1975).
[18] E. Arimondo, M. Inguscio, and P. Violino, Rev. Mod. Phys. **49**, 31 (1977).
[19] T. F. Gallagher and W. E. Cooke, Phys. Rev. A **20**, 670 (1979).
[20] L. K. Lam, R. Gupta, and W. Happer, Phys. Rev. A **21**, 1225

(1980).
[21] D. P. Aeschliman, J. Quant. Spectrosc. Radiat. Transf. **25**, 221 (1981).
[22] C. M. Huang and C. C. Wang, Phys. Rev. Lett. **46**, 1195 (1981).
[23] C. C. Wang and B. Shirinzadeh, Phys. Rev. A **28**, 1166 (1983).
[24] M. Glódź and M. Kraińska-Miszczak, J. Phys. B **18**, 1515 (1985).
[25] D. J. Hart and J. B. Atkinson, J. Phys. B **19**, 43 (1986).
[26] R. W. Berends, W. Kedzierski, J. B. Atkinson, and L. Krause, Spectrochim. Acta, Part B **43**, 1069 (1988).
[27] A. Sieradzan, R. Stoleru, W. Yei, and M. D. Havey, Phys. Rev. A **55**, 3475 (1997).
[28] H. Wang, J. Li, X. T. Wang, C. J. Williams, P. L. Gould, and W. C. Stwalley, Phys. Rev. A **55**, R1569 (1997).
[29] S. Falke, E. Tiemann, C. Lisdat, H. Schnatz, and G. Grosche, Phys. Rev. A **74**, 032503 (2006).
[30] R. Schmieder, A. Lurio, and W. Happer, Phys. Rev. A **3**, 1209 (1971).
[31] H. P. Kelly, R. L. Chase, G. R. Daum, and J. J. Chang, Phys. Rev. A **8**, 2777 (1973).
[32] T. Lee, T. P. Das, and R. M. Sternheimer, Phys. Rev. A **11**, 1784 (1975).
[33] A. Lindgard and S. E. Nielsen, At. Data Nucl. Data Tables **19**, 533 (1977).
[34] G. D. Mahan, Phys. Rev. A **22**, 1780 (1980).
[35] C. E. Theodosiou, Phys. Rev. A **30**, 2881 (1984).
[36] P. F. Gruzdev and G. S. S. A. I. Sherstyuk, Opt. Spectrosc. **71**, 513 (1991).
[37] W. R. Johnson, Z. W. Liu, and J. Sapirstein, At. Data Nucl. Data Tables **64**, 279 (1996).
[38] J. Migdalek and Y.-Ki. Kim, J. Phys. B **31**, 1947 (1998).
[39] M. Mérawa and D. Bégué, J. Chem. Phys. **108**, 5289 (1998).
[40] A. Derevianko, W. R. Johnson, M. S. Safronova, and J. F. Babb, Phys. Rev. Lett. **82**, 3589 (1999).
[41] I. S. Lim, M. Pernpointner, M. Seth, J. K. Laerdahl, P. Schwerdtfeger, P. Neogrady, and M. Urban, Phys. Rev. A **60**, 2822 (1999).
[42] I. S. Lim, J. K. Laerdahl, and P. Schwerdtfeger, J. Chem. Phys. **116**, 172 (2002).
[43] E. Eliav, U. Kaldor, and Y. Ishikawa, Phys. Rev. A **50**, 1121 (1994).
[44] E. Eliav, M. J. Vilkas, Y. Ishikawa, and U. Kaldor, Chem. Phys. **311**, 163 (2005).
[45] W. R. Johnson, S. A. Blundell, and J. Sapirstein, Phys. Rev. A **37**, 307 (1988).
[46] Yu. Ralchenko, F.-C. Jou, D. E. Kelleher, A. E. Kramida, A. Musgrove, J. Reader, W. L. Wiese, and K. Olsen (2005). NIST Atomic Spectra Database (version 3.0.2) [Online]. Available: http://physics.nist.gov/asd3 [2006 January 4]. National Institute of Standards and Technology, Gaithersburg, MD.
[47] W. R. Johnson, U. I. Safronova, A. Derevianko, and M. S. Safronova, Phys. Rev. A **77**, 022510 (2008).
[48] L. W. Fullerton and G. A. Rinker, Jr., Phys. Rev. A **13**, 1283 (1976).
[49] P. J. Mohr, Ann. Phys. (N.Y.) **88**, 26 (1974).
[50] P. J. Mohr, Ann. Phys. (N.Y.) **88**, 52 (1974).
[51] P. J. Mohr, Phys. Rev. Lett. **34**, 1050 (1975).
[52] M. S. Safronova, W. R. Johnson, and U. I. Safronova, Phys. Rev. A **53**, 4036 (1996).
[53] M. S. Safronova, W. R. Johnson, and U. I. Safronova, J. Phys. B **30**, 2375 (1997).
[54] B. Arora, M. S. Safronova, and C. W. Clark, Phys. Rev. A **76**, 052516 (2007).
[55] U. I. Safronova, M. S. Safronova, and W. R. Johnson, Phys. Rev. A **71**, 052506 (2005).
[56] W. R. Johnson, Z. W. Liu, and J. Sapirstein, At. Data Nucl. Data Tables **64**, 279 (1996).
[57] A. Derevianko and E. D. Emmons, Phys. Rev. A **66**, 012503 (2002).
[58] D. Jiang, B. Arora, and M. S. Safronova, Phys. Rev. A **78**, 022514 (2008).
[59] A. Kreuter *et al.*, Phys. Rev. A **71**, 032504 (2005).
[60] E. Iskrenova-Tchoukova and M. S. Safronova, Phys. Rev. A **78**, 012508 (2008).
[61] S. G. Porsev and A. Derevianko, J. Chem. Phys. **119**, 844 (2003).
[62] W. R. Johnson, D. Kolb, and K.-N. Huang, At. Data Nucl. Data Tables **28**, 333 (1983).
[63] W. R. Johnson, D. R. Plante, and J. Sapirstein, Adv. At., Mol., Opt. Phys. **35**, 255 (1995).
[64] URL=http://www.webelements.com.
[65] K. Beloy, U. I. Safronova, and A. Derevianko, Phys. Rev. Lett. **97**, 040801 (2006).